Research of Relationship Between Tensile Mechanical Properties of 45 Steel Laser-Hardened Surfaces and Fracture Fractal Dimension

Liu Anzhong[1] Zhang Su[1] Ding Kewei[1] Lei Sheng[2]

[1]*School of Civil Engineering, Anhui Jianzhu University, Hefei, Anhui* 230601, *China*

[2]*School of Mechanical and Electrical Engineering, Anhui Jianzhu University, Hefei, Anhui* 230601, *China*

Abstract In this study, 45 steel tensile specimens were hardened by laser during a surface experiment that used different laser power strengths, whereas the ultimate tensile strength of each specimen was obtained during a tensile experiment. These experiments measured the depth and hardness of the hardening layers of the surface areas and logged fracture photographs using a scanning electric microscope (SEM) to perform the fractal analysis. The fracture showed fractal characteristics; therefore, fractal theory was applied to calculate the fractal dimension of the fracture. The conclusive research results show that the sample surface-hardening layer depths and surface hardness can be increased by increasing the laser power, and thus causes the gradual decrease of the ultimate tensile strength and the increase of the fracture fractal dimension. The ultimate tensile strength and the fracture fractal dimension can be characterized for this material type.

Key words laser hardened; mechanical properties; tensile fracture; fractal dimension

OCIS codes 140.3390; 100.2960: 160.3900

45号钢表面激光硬化拉伸力学性能与断口分形维数关系的研究

刘安中[1] 张 速[1] 丁克伟[1] 雷 声[2]

[1]安徽建筑大学土木工程学院, 安徽 合肥 230601

[2]安徽建筑大学机械与电气工程学院, 安徽 合肥 230601

摘要 采用激光相变硬化技术对45号钢拉伸试样表面进行处理,通过拉伸实验获得试样的强度极限,测量了硬化层深度和硬化表面硬度,并用电子显微镜(SEM)对断口表面进行了分形分析,断面具有分形特征,利用分形理论计算了断面的分形维数。研究结果表明,随着激光束功率的增大,试样表面硬化层的深度和硬度是增加的,导致拉伸强度极限逐渐降低,断面分形维数也随之增大。对于该种材料,拉伸强度极限与断口分形维数可以互相表征。

关键词 激光硬化; 力学性质; 拉伸断口; 分形维数

中图分类号 TG161 **文献标识码** A

doi: 10.3788/LOP53.011401

1 Introduction

Laser-quenching techniques have been widely used in all modern manufacturing industries. The important components of a machine have been processed by laser-quenching technique, which has become a commonly used method in recent years. The advantages of laser quenching include uniformity of thickness distribution of the surface-hardened layer, high hardness, wear resistance, small work-piece deformation, and easy control[1-8].

Mechanical properties are related to the fracture-surface shape. Quantitatively describing the surface shape has been an engineering problem. The fractal theory provides a truly effective method for quantitative

收稿日期: 2015-03-25; **收到修改稿日期**: 2015-04-15; **网络出版日期**: 2015-12-28

基金项目: 国家自然科学基金(11472005)

作者简介: 刘安中(1958—),男,硕士,教授,主要从事工程力学方面的研究。E-mail: anzhongliu@126.com

analysis of the surface. Thereafter, research results have concluded that a material surface possesses statistical self-similarities within a specific scope, a discovery that concurs with the basis of the fractal theory. Many research results have shown that the mechanical properties of materials are related to the fracture fractal dimension[9-12].

In the current study, the surfaces of 45 steel tensile specimens were quenched by different laser power strengths to obtain the tensile mechanical properties of the test specimen. The fractal dimensions of the tensile fractures were obtained by applying the fractal theory, whereas the relationships among mechanical properties of the tensile specimen of the 45 steel quenched by laser and the fracture fractal dimension were discussed.

2 Material treatment and experimental procedures

2.1 Material surface treatment

The tensile specimens were made of 45 steel, and the size of each rectangular cross section of the specimen was 20 mm×5 mm. After a thorough acetone cleaning, the surface of each specimen was subjected to black organic spray coating. Then, laser treatment was performed using a 3.0 kW CFTQ-2-type precision computer numerical control (CNC) laser-machine system, as shown in Fig.1. The tensile specimens in the middle were treated by laser-beam power of 900, 1300, and 1500 W. The laser focus area was 15 mm × 1 mm, and the scanning speed was 700 mm/min .

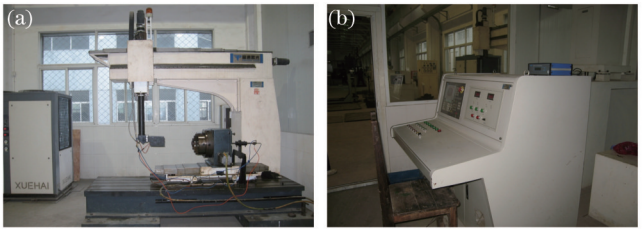

Fig.1 GFTQ-2-type precision CNC laser-machine system. (a) Workbench; (b) control system

2.2 Tensile experiment

The tensile experiment was performed using a WDW-100 electronic universal testing machine, as shown in Fig.2 (a). The tensile-tested specimens are shown in Figs.2 (c) and 2 (d). The load deformation curve is

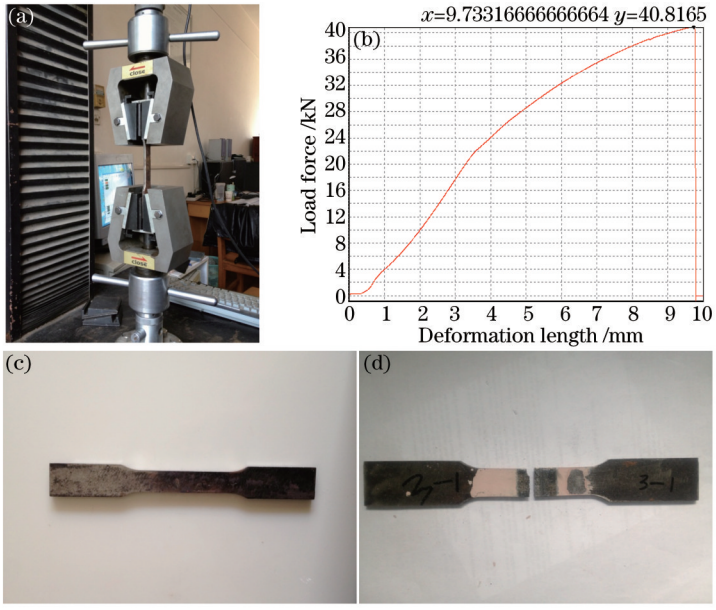

Fig.2 Tensile experiment. (a) WDW-100 electronic universal testing machine;
(b) sample 3-1 tensile load deformation curve; (c) tensile standard sample; (d) tensile failure sample

also shown in Fig.2 (b). The experimental results conclude that the sample surface-hardening layer depth and surface hardness increase with the increase of the laser power. However, the ultimate tensile strength gradually decreases with the increase of the laser power.

Table 1 Experimental data of the 45 steel samples hardened by laser

Sample number	1	2	3	4
Beam power /W	1500	1300	1100	900
Ultimate strength /MPa	407.57	410.208	419.98	434.524
Depth of hardened layer /mm	0.228	0.195	0.168	0.138
Hardness /HRC	67.2	65.9	64.9	62.2

The experimental results are listed in Table 1. According to the experimental results listed in Table 1, the relationship between the ultimate strength and laser beam power can be obtained, which is shown in Fig.3. In addition, the approximate fitting formula for the relationship between the laser beam power and ultimate strength can be obtained as follows:

$$\sigma_b = 7\times10^{-5}P^2 - 0.2239\times10^{-2}P + 575.88\,. \tag{1}$$

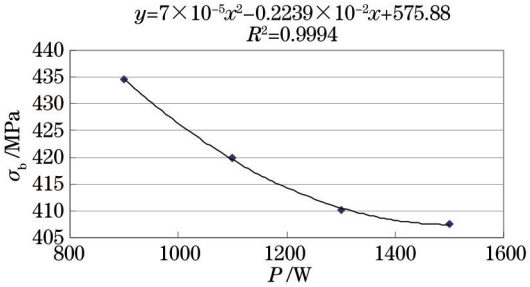

Fig.3 Relationship between ultimate strength σ_b and laser power P

2.3 Metallographic analysis

The strengthening characteristics of the test specimen are generally related to the overall surface hardness of the alloys and the micro-structural characteristics of the laser-quenched layer of the specimen.

The 45 steel sample surface was then heated above the austenitization temperature by laser-heating treatment. Subsequently, rapid cooling due to the self-quenching property of the specimen led to the formation of a hardened surface layer containing carbides in a matrix of austenite and martensite. The results indicate that the hardness of the laser-quenched layer is substantially higher than those resulting from conventional heat treatment. The hardness enhancement of the hardened layer is attributed to grain refining and the formation of supersaturated (yet hidden) crystal martensite during wide-band laser quenching. The hardened layer of the laser-treated block was 0.13~0.25 mm thick.

The hardness gradient of the hardened layer showed a gradual decrease in hardness, which is likely due to the reduced dissolution of carbide that results from a temperature gradient found in the depth direction. Therefore, the depth of the hardened layer increases with the increase of the laser power. The increase of the laser power also causes the depth of the hardened layer to spike in accordance with the amount of laser power. When the laser output power increases, the metal surface that absorbs the energy subsequently increases, further improving the temperature of the metal surface after the rapid transfer matrix. The area of the metal surface in the phase-change temperature above Ac3 also increases, which eventually leads to the increase of the depth of the hardened layer. The increase of the depth of the hardened layer and the surface hardness causes a fracture-zone stress state change, leading to the decrease of the tensile strength.

3 Fractal analysis of the laser-hardened tensile fractures

The scanning electric microscope (SEM) picture of the tensile fractures shows that the fracture surface has statistical self-similarities within a certain scope. Fractal characteristics are also present on the tensile-

fracture surface, as shown in Fig.4. The micro-structure of the fracture surface could be tested by applying the fractal theory. The SEM picture of the fracture surface could be quantitatively described by the fractal dimension of the surfaces.

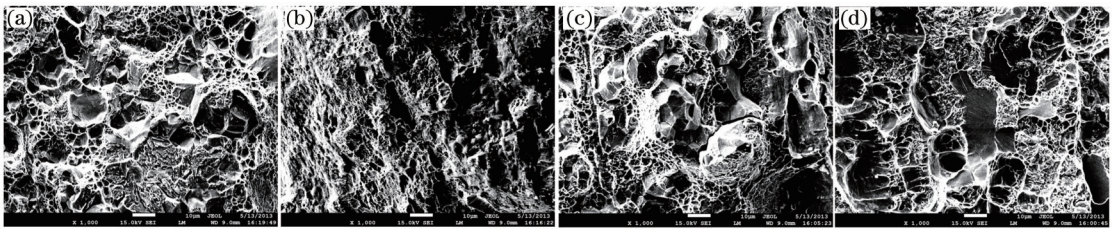

Fig.4 SEM pictures of the tensile fracture. (a) 900 W; (b) 1100 W; (c) 1300 W; (d) 1500 W

First, the gray values of the SEM picture were obtained using an image-processing technique, and they were used to replace the high values of the fracture surface. By using a cubic box to cover the fracture surface, the SEM picture of the fracture surface could be adjusted into the grid. The size of the cubic box is $\delta_n \times \delta_n \times h_n$, where δ_n is the grid size and h_n is the height of the cubic box, respectively. The fractal dimensions of the fracture surface were calculated according to the box-dimension method.

$$N_\delta(F) = C\delta_n^{-D}, \tag{2}$$

Where F represents the surface, and $N_\delta(F)$ is the the number of the cover box. C is a constant, and D is the fractal dimension of the surface. Taking the logarithm of Equ. (2), we can obtain

$$\lg N_\delta(F) = -D \lg \delta_n + \lg C . \tag{3}$$

When the grid size is changed, the logarithmic curve is obtained, as shown in Fig.5. According to the slope of the logarithmic curve, the fractal dimension of the fracture surface is obtained, as listed in Table 2.

Table 2 Fractal dimension D of the tensile-fracture surface

Sample number	1	2	3	4
Beam power /W	1500	1300	1100	900
Fractal dimension	2.7731	2.7571	2.7494	2.7404

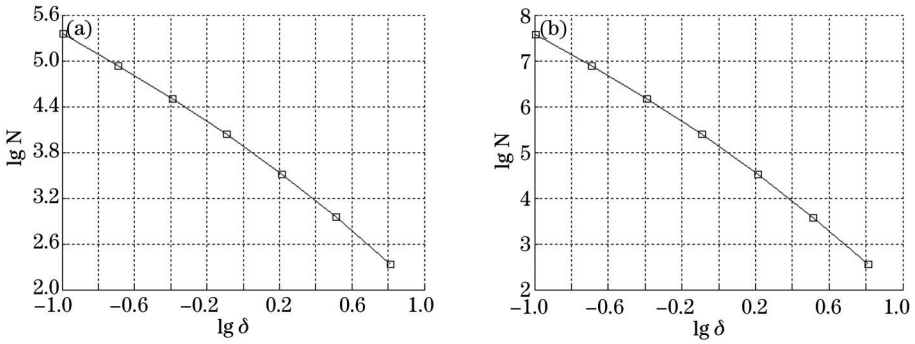

Fig.5 Fractal-dimension logarithmic curve. (a) Sample 3-1; (b) sample 3-3

The above graphs show that as the laser power begin to change, the fractal dimension also changes accordingly. The experimental results listed in Table 2 show that the relationship between fractal dimension D of the tensile fracture and laser power P can be obtained, as shown in Fig.6 (a). The approximate fitting formula of the relationship between P and D is obtained as follows:

$$D = 4 \times 10^{-8} P^2 - 5 \times 10^{-5} P + 2.75 . \tag{4}$$

According to the experimental results listed in Tables 1 and 2, the relationship between the ultimate strength and the fractal dimension of the tensile fracture can be obtained, as shown in Fig.6 (b). The approximate fitting formula of the relationship between σ_b and D is obtained as follows

$$\sigma_b = 1 \times 10^6 D^3 - 9 \times 10^6 D^2 + 2 \times 10^7 D - 2 \times 10^7 . \tag{5}$$

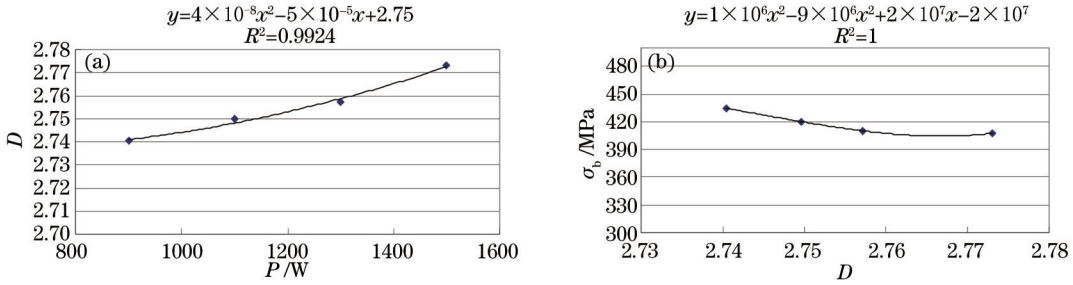

Fig.6 (a) Relationship between fractal dimension D and laser power P; (b) relationship between ultimate strength σ_b and fractal dimension D

4 Conclusion

1) When 45 steel tensile specimens are laser-hardened with increased laser power, the depth of the hardened layer and the surface hardness increase, but the ultimate tensile strength decreases.

2) When the laser-hardened 45 steel tensile specimens are tested, a relationship between the ultimate tensile strength and the fracture fractal dimension is obtained. We can estimate the ultimate tensile strength according to the fracture fractal dimension.

3) For the laser-hardened 45 steel tensile specimens, the SEM pictures show that the tensile-fracture surface has a statistical self-similarity within a certain scope. The fractal dimension can be used to describe the fracture-surface shape. With the increase of the laser power, the fracture-surface fractal dimension increases.

References

1 Cheng Yiyuan, Wang Yong, Han Bin, *et al*.. Microstructure and properties of 35CrMoAL steel in laser quenching nitriding [J]. Chinese J Lasers, 2010, 37(1): 250-255.
程义远, 王 勇, 韩 彬, 等. 35CrMoAL 钢激光淬火-渗氮复合处理微观组织与性能[J]. 中国激光, 2010, 37(1): 250-255.

2 Yuan Ling, Ren Xudong, Yan Gang, *et al*.. Experimental study of laser-generated surface acoustic waves in laser shock hardening metals[J]. Chinese J Lasers, 2008, 35(1): 120-124.
袁 玲, 任旭东, 严 刚, 等. 激光冲击硬化层中激光声表面波的实验研究[J]. 中国激光, 2008, 35(1): 120-124.

3 Hao Qiaoling, Shen Chaoying, Wang Shouzhong. Study on laser surface hardening of piston ring groove[J]. Hot Working Technology, 2009, 38(6): 150-152.
郝巧玲, 申超英, 王守忠. 活塞环槽的激光表面硬化研究[J]. 热加工工艺, 2009, 38(6): 150-152.

4 Chen Xiyuan, Shen Chang′an. Characteristic of laser case hardening and its application advantage in gear and mould [J]. Heat Treatment Technology and Equipment, 2012, 33(2): 4-14.
陈希原, 沈长安. 激光表面硬化的特点及在齿轮和模具中的应用优势[J]. 热处理技术与装备, 2012, 33(2): 4-14.

5 Song Liping. Laser surface modification and application[J]. Physics and Engineering, 2010, 20(4): 42-44.
宋立平. 激光表面改性及其应用[J]. 物理与工程, 2010, 20(4): 42-44.

6 Lei Sheng, Liu Quankun, Miao Xianwen, *et al*.. Influence of the laser transformation hardened layers on the flexural properties of GCr15 steel components[J]. Transactions of Materials and Heat Treatment, 2010, 31(5): 132-135.
雷 声, 刘全坤, 缪宪文, 等. 激光硬化层对 GCr15 钢弯曲性能的影响[J]. 材料热处理学报, 2010, 31(5): 132-135.

7 Zhang Peilei, Ding Min, Yao shun, *et al*.. Research of laser transformation hardening on mild steel[J]. Laser Technology, 2009, 33(6): 586-589.
张培磊, 丁 敏, 姚 舜, 等. 低碳钢表面激光相变硬化研究[J]. 激光技术, 2009, 33(6): 586-589.

8 Duan Yanli, He Huan, Fu Yuechun, *et al*.. Research progress in laser surface modification of alloys[J]. Materials Review, 2010, 24(z2): 205-207.
段艳丽, 何 欢, 符跃春, 等. 合金激光表面改性的研究进展[J]. 材料导报, 2010, 24(专辑 16): 205-207.

9 Tang Wei, Zhu Hua, Wang Yong. Fractal behavior of stress corrosion fracture[J]. Journal of Iron and Steel Research, 2007, 19(8): 56-58.

唐 玮, 朱 华, 王 勇. 应力腐蚀断口的分形行为[J]. 钢铁研究学报, 2007, 19(8): 56-58.

10 Wu Chengbao, Liang Jizhao. Fracture-surface fractal dimension of PP/diatomite composites and its relation to impact strength[J]. Journal of South China University of Technology (Natural Science Edition), 2009, 37(8): 150-154.
吴成宝, 梁基照. PP/硅藻土复合材料断口分形维数及其与冲击强度的关系[J]. 华南理工大学学报(自然科学版), 2009, 37(8): 150-154.

11 Feng Jie, Tan Yun, Tao Ping, *et al.*. Effects of inner hydrogen on fracture fractal dimension of austenitic stainless steels tensile specimens[J]. Materials Review, 2014, 28(2): 118-121.
丰 杰, 谭 云, 陶 萍, 等. 内部氢对奥氏体不锈钢拉伸断口分形维数的影响[J]. 材料导报, 2014, 28(2): 118-121.

12 Manderlbrot B B, Passoja D E, Paullay A J. Fractal character of fracture surface of metals[J]. Nature, 1984, 308(5961): 721-724.

栏目编辑: 殷建芳